Blood Interactions with Noble Metals: Coagulation and Immune Complement Activation

Mats Hulander,*,† Jaan Hong,‡ Marcus Andersson,† Frida Gervén,† Mattias Ohrlander,§ Pentti Tengvall,|| and Hans Elwing†

Department of Cell and Molecular Biology/Interface Biophysics, Gothenburg University, Medicinaregatan 9E, 41390 Gothenburg, Sweden, Division of Clinical Immunology, Uppsala University, SE-751 05 Uppsala, Sweden, Bactiguard AB, 102 42 Stockholm, Sweden, and Department of Biomaterials Science, Sahlgrenska Academy, Gothenburg University, Medicinaregatan 9E, 41390 Gothenburg, Sweden

ABSTRACT Noble metals are interesting biomaterials for a number of reasons, e.g., their chemical inertness and relative mechanical softness, silver's long known antimicrobial properties, and the low allergenic response shown by gold. Although important for the final outcome of biomaterials, little is reported about early events between pure noble metals and blood. In this article, we used whole blood in the "slide chamber model" to study the activation of the immune complement activation, generation of thrombin/antithrombin (TAT) complexes, and platelet depletion from blood upon contact with silver (Ag), palladium (Pd), gold (Au), titanium (Ti), and Bactiguard, a commercial nanostructured biomaterial coating comprised of Ag, Pd, and Au. The results show the highest TAT generation and platelet depletion on Ti and Au and lower on Pd, Ag, and the Bactiguard coating. The immune complement factor 3 fragment (C3a) was generated by the surfaces in the following order: Ag > Au > Pd > Bactiguard > Ti. Quartz crystal microbalance adsorption studies with human fibrinogen displayed the highest deposition to Ag and the lowest onto the Bactiguard coating. The adsorbed amounts of fibrinogen did not correlate with thrombogenicity in terms of TAT formation and platelet surface accumulation in blood. The combined results suggest, hence, that noble metal chemistry has a different impact on the protein adsorption properties and general blood compatibility. The low thrombogenic response by the Bactiguard coating cannot be explained by any of the single noble metal properties but is likely a successful combination of the nanostructure, nanogalvanic effects, or combinatory chemical and physical materials properties.

KEYWORDS: silver • palladium • gold • titanium • immune complement • protein adsorption • coagulation • platelets • nanostructure • QCM-D

1. INTRODUCTION

1.1. Noble Metals. Along with the development of new implant applications, there is a growing need for highly specialized materials with improved biological adaptation. This pushes biomaterials science toward new frontiers. Metals have been used for centuries in medical applications and are today common in many demanding load-bearing dental and orthopedic applications, either as pure solids or in alloys. Noble metals are used because of their ability to resist corrosion at physiological conditions and their advantageous mechanical properties. Titanium (Ti) is the least noble metal in the current experimental setup and has been used as a biomaterial since the 1970s because of its superior integration in bone, especially in dental applications (1). Silver (Ag) is used because of its recognized antibacterial properties and is deposited onto a variety of items, e.g., urinary catheters and wound dressings (2, 3). The genotoxic and cytotoxic effects of released Ag from surgery fixation pins was studied in vitro by Bosetti et al., and they concluded that Ag was much more toxic toward bacteria than toward the tested human cells (4). However, proliferation and cell survival of NIH3T3 mouse fibroblasts and human embryonic epithelial lung cells (L132), respectively, are affected by Ag, although to moderate levels, as described in ref 5. Pure palladium (Pd) has until now few medical applications but can be found as a radioactive isotope in brachytherapy and in dental alloys (6, 7). Few data are available regarding the cytotoxicity of pure Pd. Hornez and co-workers found no cytotoxicity of Pd in a thorough study on dental implant alloys (5), when compared to a wide range of other metals. Gold (Au) has been used for centuries as a biomaterial although today the medical applications are few. Its largest application area is as jewelry, in dentistry, and in brachytherapy, although new applications may show up in the near future by utilization of nanoparticles in drug release and sensor systems (6, 8). Au is generally considered an inert metal and is more common in, e.g., biosensors because of its electrical conductivity and low solu-

* Corresponding author. Tel.: +46-31-7862584. Fax: +46-31-7862599. E-mail: mats.hulander@cmb.gu.se.

Received for review January 12, 2009 and accepted April 20, 2009

† Department of Cell and Molecular Biology/Interface Biophysics, Gothenburg University.

‡ Uppsala University.

§ Bactiguard AB.

|| Department of Biomaterials Science, Sahlgrenska Academy, Gothenburg University.

DOI: 10.1021/am900028e

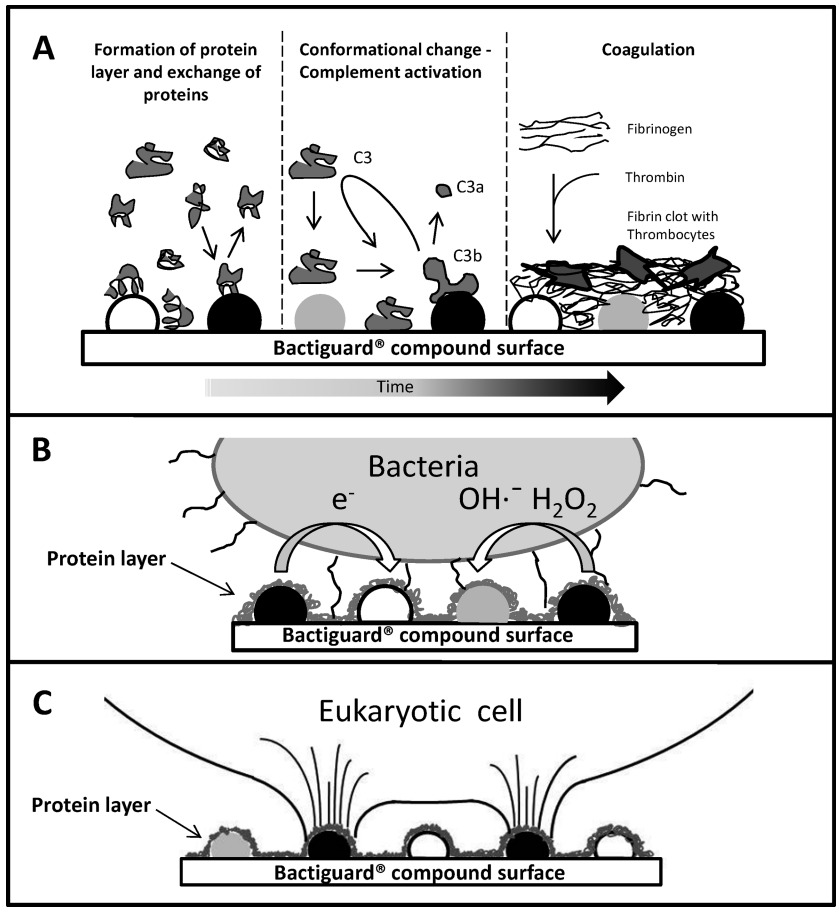

FIGURE 1. Schematic view of the three proposed hypotheses regarding the bioresponse on the Bactiguard coating. (A) General protein adsorption onto a solid surface when exposed to the physiological milieu. In blood, immune complement activation and the attachment of platelets also occur at an early stage. (B) Bactericidal effect of the Bactiguard coating through a proposed nanogalvanic action or the production of ROS at the surface, both powered by the electrochemical difference between the noble metals in the coating. (C) Increased biocompatibility and preservation of the immune system on the Bactiguard coating by eukaryotic cell attachment to the nanostructure.

bility. The cytotoxic effect of Au in its ground state is negligible because Au is used, e.g., in jewelry and even in food. However, salts of Au are known to be of immunological and cytotoxic relevance (9).

1.2. Bactiguard Coating. The Bactiguard coating is comprised of nanosized deposits of Ag, Pd, and Au. The coating is in clinical use on urinary catheters (Bardex IC, LubraSil IC, Bard Medical, Covington, GA, and BIP foley, Bactiguard AB, Stockholm, Sweden) and has been shown to significantly reduce catheter-associated urinary tract infections (CAUTI) in clinical trials (10). The coating is also clinically tested on central venous catheters with successful prevention of catheter-related infections apparently without compromising biocompatibility (11). The coating can be applied to a large variety of substrates including glass, metal, and polymer surfaces. However, the details regarding the coating's interactions with plasma proteins or whole blood are not yet fully understood. Two desired features of a blood contacting device are low immune complement activation and low thrombogenicity because these factors can have a profound systemic impact in, e.g., transfusional medicine and dialysis. Therefore, in vitro studies are needed to understand the response of blood to the coating and possibly the mechanism of action behind the observed responses of the Bactiguard coating.

In order to facilitate research on physiological and biological responses observed on this coating, we propose three major hypotheses to explain its mode of interaction; see Figure 1a–c (not to scale). A schematic view regarding early events on a biomaterial in a physiological milieu is shown in Figure 1a. Proteins rapidly become adsorbed onto the solid surface. This phenomenon is a general feature that companions all of the below hypotheses and is therefore of basic relevance throughout the whole process of implant/biomaterial–host interactions. In addition, protein adsorption in blood also results in immune complement deposition and eventually the attachment of platelets to fibrin or fibrinogen.

The second hypothesis, illustrated in Figure 1b, addresses the antimicrobial properties of the coating. It is a general conception that most bacteria attach to surfaces through interactions with preadsorbed proteins. Therefore, we find it unlikely that bacteria attach directly onto the Bactiguard coating but rather to plasma proteins that adsorb quickly to the coating. Once attached, the bacteria may be subjected to a nanogalvanic current powered by the difference in the electrochemical potential between the metal nanosized grains. This tentative antimicrobial nanogalvanic action was recently proposed by Chiang et al. (12). Related to the above hypothesis is an antibacterial mechanism proposed by

Table 1. Representative Amounts of Ag, Pd, and Au Present in the Bactiguard Coating on QCM-D Crystals and on PVC Medical Tubing Used in the Experiments

	Ag (μg/cm^2)	Pd (μg/cm^2)	Au (μg/cm^2)
QCM-D	0.46	0.02	0.09
PVC	0.36	0.35	0.15

Chang et al. (13), where the electrochemical difference between Ag nanoparticles and Al_2O_3 is thought to drive the conversion of O_2 to yield the reactive oxygen ion $O_2^{\bullet -}$. The presence of $O_2^{\bullet -}$ at the surface will then give rise to additional reactive oxygen species (ROS) like $OH^{\bullet -}$ or H_2O_2. Thus, the bactericidal effect is proposed to originate from the oxidative damage by ROS to the bacteria rather than from Ag itself. It is possible that the differences in the electrode potential between the different metals in the Bactiguard coating could induce the same mechanism as that proposed by Chang and co-workers. Although Ag ions are known to be toxic to bacteria, it is unclear whether the minute amounts of Ag in the Bactiguard coating (see Table 1) are sufficient to completely explain its antimicrobial properties.

The third hypothesis concerns the eukaryotic compatibility of the coating and is illustrated in Figure 1c; we hypothesize that either the nanostructure of the coating or the chemistry of the single nanoparticles (or both) could affect cell attachment. It is known that proteins that adsorb to a certain structure or to a structure with certain chemistry can undergo conformational changes (14, 15). When the conformation of the protein is altered, certain epitopes of the protein that signal for cell attachment (e.g., the well-known RGD sequence) may be exposed. Cells (e.g., eukaryotic phagocytotic cells) would then "choose" or prefer to attach onto these structures (see also the Discussion section). The eukaryotic compatibility of the Bactiguard would then be a consequence of adsorbed proteins that have undergone conformational changes. This proposed mechanism could per se explain much of the low tendency of CAUTI associated with the Bactiguard coating. Here we have chosen to study the immune complement activation and blood coagulation on each individual pure noble metal and the Bactiguard coating because these are central and early established processes that will affect subsequent tissue response and integration. A brief introduction to protein adsorption, immune complement activation, and blood coagulation is presented below.

1.3. Protein Adsorption. Although generally agreed that protein adsorption is an important feature during early host response, coagulation rate, cell adhesion, and tissue integration, surprisingly little is reported about how this dictates cell response and eventual implant success. Within seconds or minutes upon introduction to a tissue or body fluid, complex protein cascade systems begin to interact at or with the biomaterial surface (16–19). The protein adsorption exerted on the surface is a dynamic process where smaller proteins (like, e.g., albumin) rapidly adsorb to the surface and may be followed by, and eventually replaced by, other ones in the phenomenon described as the Vroman effect (20, 21). Hence, in an implant situation, cells will not primarily attach to the surface but rather to adsorbed proteins (16, 19, 22). It is well established that hydrophobicity, chemistry, and surface topography are crucial factors of protein adsorption (23–28) and that these parameters also affect cell adhesion (16, 29). The understanding of early adsorption events on a biomaterial is of great importance for the understanding, and possibly the manipulation, of integration and inflammation.

1.4. Immune Complement. The immune complement system comprises about 30 different plasma proteins and is a finely tuned and regulated system responsible for host protection against foreign or "non-self" matter and against invading microorganisms through the formation of the terminal complement complex, i.e., generation of cell lysis. The complement system is divided into the classical, lectin, and alternative pathways. The classical pathway requires activation by antibodies and is generally not considered the most important for the immune response at biomaterials. However, nonspecific binding of antibodies to a biomaterial surface can indeed trigger the activation of the immune complement system through this pathway (30). The lectin pathway is partly common with the classical pathway and is initiated by certain lectin structures, many of which have been identified at bacterial surfaces. It is not considered important for biomaterials. The activation of the alternative pathway occurs when C3 splits spontaneously into C3b* and C3a. The thiol ester part of C3b* is reactive and may, in turn, bind to (protein-coated) surfaces or be inactivated to iC3b by reaction with water (31). Measurement of these components of the complement system is shown to correlate with acute inflammation caused by a biomaterial (32). For a more detailed reading on the immune complement activation and its mechanisms, we suggest the article by Gros et al. (33).

1.5. Blood Coagulation. The blood coagulation cascade is a host defense system that maintains the integrity of the body's blood vessels. It is divided into extrinsic and intrinsic pathways and is comprised of some 20 plasma proteins. Both pathways share the terminal part of the cascade, where fibrinogen is finally converted into fibrin in order to create a fibrin clot that together with blood cells form a plug that prevents hemorrhage at the site of damage. The extrinsic pathway is activated by tissue factor (TF) secreted by cells surrounding the damaged area, and there is evidence that this pathway is involved in biomaterial-associated coagulation as well. The intrinsic pathway is considered the most important in biomaterial-associated coagulation and is triggered by the activation of factor XII and high-molecular-weight kininogen (HMWK) upon spontaneous adsorption to negatively charged surfaces. The coagulation cascade is a tightly regulated system in order to prevent unwanted or excess clot formation. The conversion of fibrinogen to fibrin by thrombin is, for example, regulated by the formation of the complex thrombin/antithrombin (TAT), in which thrombin is disabled through blocking of its active site (31). The concentration of this complex is an

appropriate indicator of the overall activation of the coagulation system because the occurrence of thrombin in high concentrations reflects an activation of the intrinsic coagulation pathway (34). Interactions are now being confirmed between the immune complement and coagulation cascades, making the understanding of biomaterial-associated coagulation and inflammation an even more complex issue. Further reading on the coagulation system and it's regulation is available in a comprehensive article by Monroe and Hoffman (35).

1.6. Aim. By use of carefully prepared noble metal surfaces and by combination of the quantum-classical molecular dynamics (QCM-D) techniques with the slide chamber model, our aim in this work was to investigate the impact of noble metal chemistry on early protein adsorption and how this may affect the immune complement and blood coagulation systems. We also wanted to single out whether any (if so) of the noble metals in the Bactiguard coating could be responsible for the unique low-interaction features of this noble metal coating.

2. MATERIAL AND METHODS

2.1. Blood Products. Blood was drawn from one apparently healthy donor into a 50-mL heparinized Falcon vial containing soluble heparin (Leo Pharma A/S, Ballerup, Denmark) to give a final concentration of 1.0 IU heparin/mL. The blood was used immediately (within minutes) after sampling. Human fibrinogen was obtained from Sigma-Aldrich and diluted in veronal buffer saline (VBS^{2-}; i.e., without $CaCl_2$ and $MgCl_2$) to a final concentration of 1 mg/mL.

2.2. Surface Preparations. The respective noble metal was physical vapor deposition (PVD)-deposited (5×10^{-6} mbar, Linköping University, Linköping, Sweden) to standard microscope glass slides or QCM-D sensor crystals to a thickness of approximately 150 nm on top of a supportive layer of 35 Å chromium (Cr). For the QCM-D experiments with Au and Ti, Q-Sense's standard Au and Ti sensor crystals (QSX 301 and QSX 310, respectively) were used.

The Bactiguard coating was applied to poly(vinyl chloride) (PVC) medical tubing (BioLine, Luckenwalde, Germany) or to standard SiO_2 QCM-D sensor crystals QSX303 (Q-Sense, Västra Frölunda, Sweden) through Bactiguard AB's standard coating protocol. The coating procedure involves a series of up to 21 wet-dipping steps, briefly described here; the surface was first pretreated by immersion in chromic acid (H_2CrO_4), followed by rinsing in Milli-Q water. Activation of the surface was then obtained by immersion in an aqueous solution of stannous chloride ($SnCl_2$) and then additional rinsing in Milli-Q water. The substrate was then plated with a uniform layer of Ag by immersion in silver nitrate ($AgNO_3$), after which rinsing with Milli-Q water was performed again. Au and Pd were then subsequently deposited by immersion of the substrate, a dilute suspension of Au and Pd nanoparticles, obtained through the reduction of solutions of Au and Pd salts and the addition of a stabilizing agent. The coating process results in a heterogeneous deposition of particles ranging in size between 10 and 100 nm. The amount and size of the particles can be controlled by, e.g., varying the amount of reducing agent and/or stabilizer in the solutions. The nanotopography of the Bactiguard coating can be viewed in the atomic force microscopy (AFM) data in Figure 2. A more detailed description of the coating procedure can be found in U.S. Patent 2007/0237945 A1.

Prior to the experiments, all surfaces, except Ag and Bactiguard, were treated in a UV/O_3 chamber for 15 min. Au surfaces were then immersed in a 5:1:1 solution of Milli-Q water, 25% NH_3 (reagent grade, Scharlau), and 30% H_2O_2 (Fluka) for at least 30 min at 80 °C. Pd and Ti surfaces were instead immersed in 50 mM sodium dodecyl sulfate [20% (w/v), Calbiochem] for at least 1 h at 80 °C. After washing in an excess of Milli-Q water and drying with N_2(g), the surfaces were again treated in the UV/O_3 chamber for 20 min. The Ag surfaces were treated with Ar plasma [Technics Plasma 440G (IPF, Göteborg, Sweden)] at 300 W at 0.7 mbar for 2 s and kept in Falcon vials in a N_2(g) atmosphere prior to measurements. The Bactiguard-coated surfaces were washed with an excess of Milli-Q water and dried with N_2(g) prior to the experiments.

2.3. Elemental Composition of the Bactiguard Coating. The Bactiguard-coated QCM-D sensor crystals were immersed in a solution containing 1.54 M HNO_3 and 23 mM HF. The solution was heated gradually for 15 min up to 180 °C and then kept at a constant temperature for 10 min in a Venticell 55 oven (MMM Medcenter GmbH).

The Bactiguard-coated PVC samples were dissolved in a solution containing 10.3 M HNO_3, 2.5 M HF, and 2.6 M H_2O_2 in an Anton Paar Multiwave 3000 microwave oven on a 16HF100 rotor by gradually increasing the effect to 1200 W for 14 min and then kept constant for 30 min.

The prepared solutions were subsequently analyzed for their Ag, Pd, and Au concentrations with a graphite furnace atomic absorbance spectrum analyzer (SIMAA 6100 AS 800 autosampler, Perkin Elmer Instruments, Waltham, MA). All measured data were calibrated against a standard curve obtained from diluted stock solutions of Ag, Pd, and Au, respectively (Merck), in 69% HNO_3 (BDH). The amounts of Ag, Pd, and Au in the Bactiguard coating are presented in Table 1.

2.4. Surface Analysis. 2.4.1. ***Wettability.*** The surface wettabilities were measured by the sessile water drop method. The diameter of a 10-μL droplet of Milli-Q water applied on the surfaces was measured. From these data, the contact angle of the droplet was calculated as described by Dahlgren and Sundquist (36).

2.4.2. ***Electron Spectroscopy for Chemical Analysis (ESCA).*** To assess the occurrence of airborne hydrocarbon pollutants adsorbed to the surface of our experimental surfaces, elemental analysis of the QCM-D sensor crystals was performed on a Quantum 2000 scanning ESCA microprobe from Physical Electronics. An Al Kα (1486.6 eV) X-ray source was used, and the beam size was 100 μm. The analyzed area was 500 × 500 μm and the take-off angle 45° with respect to the sample surface. The surfaces used in the slide chamber were not subject to ESCA because the preparation and handling of the surfaces prior to the experiments were identical with that of the QCM-D sensor crystals.

2.4.3. ***AFM.*** The surface topography of Ag, Pd, Au, and the Bactiguard coating was analyzed on a DI nanoscope 3000 AFM in tapping mode, using a NSC 15 standard silicon cantilever tip at a spring load constant of 50 N/m from MikroMasch USA (San Jose, CA). The analyzed area was 1 × 1 μm. Measurements were made on Ag, Pd, and Au deposited with a PVD technique onto QCM-D sensor surfaces and on the Bactiguard coating deposited on QCM-D crystals, as described in section 2.2.

2.5. Slide Chamber Model. The slide chamber model is constructed of two poly(methyl methacrylate) (PMMA) rings glued onto a PMMA slide the size of a microscope slide. In brief, the two rings form two wells with a volume of 1.65 mL each, and the test surface is placed as a lid over the two wells, creating two closed circular chambers (37). Prior to the experiments, all parts of the slide chamber (except for the surface to be tested) were heparinized using the Corline method (Corline Systems, Uppsala, Sweden) to obtain a surface concentration of 0.5 μg/cm^2. A total of 1.3 mL of blood was transferred to each well, leaving a 0.35-mL bubble of air inside each well, which functioned as a stirrer throughout the experiments. After the wells

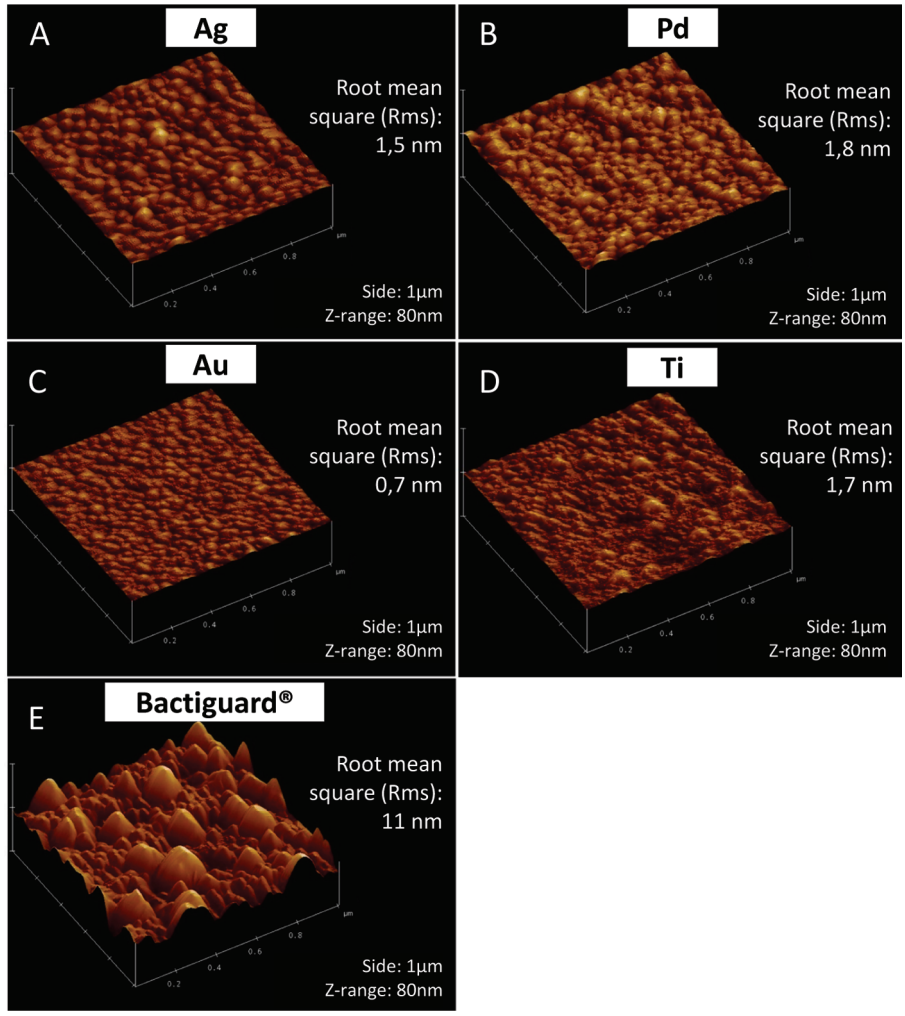

FIGURE 2. AFM micrographs of QCM-D sensor crystals deposited with (A) Ag, (B) Pd, (C) Au, (D) Ti, and (E) the Bactiguard coating. Note the difference in roughness between the pure metals and the Bactiguard coating, indicated also by the rms values.

were closed with the test surface, the slide chambers were attached to a disk with a diameter of 30 cm and rotated vertically for 60 min at 22 rpm in a 37 °C water bath.

2.6. Blood Analyses. 2.6.1. *Platelet Count.* After incubation in the slide chamber, the blood samples were gently mixed and analyzed for platelets on an automated cell counter (Coulter AcT diff, Coulter Corp., Miami, FL). The remaining blood was mixed with EDTA-K3 to a final concentration of 4 mM and centrifuged at 4600*g* for 10 min at +4 °C. The plasma was collected and stored at −70 °C prior to C3a and TAT detection (see below).

2.6.2. *Detection of C3a.* The ethylenediaminetetraacetic acid (EDTA)-treated blood plasma (see above) was diluted $^{1}/_{500}$ and analyzed in a sandwich ELISA, which employs the monoclonal 4SD17.3 capture antibody (Uppsala University, Uppsala, Sweden) (38). Bound C3a was detected with biotinylated rabbit antihuman C3a (Dako AS, Glostrup, Denmark) followed by HRP-conjugated streptavidin (Amersham Biosciences, Buckinghamshire, U.K.). Zymosan-activated serum calibrated against a solution of purified C3a served as a standard.

2.6.3. *Detection of TAT Complexes.* TAT complexes in EDTA-inactivated plasma were measured by an *in-house*-developed sandwich ELISA protocol using polyclonal antithrombin (210C) as capture antibodies and polyclonal peroxidase conjugated anti−antithrombin III (210D) as detection antibodies (both from Enzyme Research, South Bend, IN).

The protocol standard was calibrated against a commercial TAT detection ELISA kit (Enzygnost TAT micro, Behringwerke AG, Marburg, Germany). Samples were diluted with normal human plasma considered free or very low of TAT.

2.7. QCM-D Technique. The QCM technique is an acoustic method based on the piezoelectric properties of quartz crystals. The fundamental resonance frequency of the sensor crystal (in this case, 5 MHz) is found by applying an alternating current over the crystal. Mass adsorbed onto the crystal decreases the resonance frequency (Δf), which, in turn, is proportional to the adsorbed mass. The analysis depth decreases with increasing frequency and can be chosen by monitoring of the overtones produced by the oscillating crystal. The mass is calculated by the Sauerbrey equation (39):

$$M = -C\frac{\Delta f}{n} \qquad (1)$$

where M is the mass in ng/cm^2, C is the mass sensitivity constant [17.7 ng/(cm^2 Hz), for a 5-MHz sensor crystal], and n is the overtone number 1, 3,...,n. When the current is switched on and off, the dampening of the signal can be measured, and the dissipation (D) can be determined. Dissipation is a dimensionless entity yielding information about the viscoelastic properties of the adsorbed film. High dissipation indicates a higher motility and hence a loosely packed adsorbed layer, whereas a rigid and more densely packed layer yields a low dissipation. It is known that the QCM technique will overestimate the adsorbed mass when measurements are done in an aqueous solution, compared to optical-surface-sensitive methods, e.g., ellipsometry or

Table 2. Static Contact Angles of the Metals at Different Times from Washing

	contact angle	
surface	$T = 0$ h	$T = 24$ h
Ag	20 (±5)	60 (±4)
Pd	<10	47 (±5)
Au	<10	<10
Ti	<10	20 (±13)
Bactiguard (PVC tubing)	na	72 (±3)
Bactiguard (QCM-D)	na	69 (±10)

Table 3. Representative Amounts of Surface-Bound Carbon (%) Found on the Surfaces after Approximately 24 h

	Bactiguard	Ag	Pd	Au	Ti
surface-bound carbon (%)	25	23	17	21	23

optical waveguide light spectroscopy. This is due to the fact that the QCM technique measures the total amount of adsorbed mass, including water entrapped in or associated with the protein layer. The entrapped water can give rise to a high dissipation and thus give a false positive value of the adsorbed total mass when calculated with the Sauerbrey equation (eq 1) (40).

2.8. Adsorption of Fibrinogen Studied with QCM-D. The adsorption of human fibrinogen to noble metals and the Bactiguard coating was monitored at the third overtone (15 MHz) for 45 min at room temperature (22 ± 0.2 °C) and a protein concentration of 1 mg/mL. Each run was initiated with a baseline check for 5 min in a carrier buffer (VBS^{2-}). After 45 min of fibrinogen adsorption, each run was finalized with a rinsing of the surface with 1 mL of a carrier buffer for 5 min (see Figure 6). All experiments were performed on a QCM-D instrument D300 (Q-Sense, Västra Frolunda, Sweden).

2.9. Statistics. All bars in the figures represent average values and standard deviations ($N \geq 5$). All data were analyzed using single factor ANOVA with a 95% confidence interval.

3. RESULTS

3.1. Wettability (Contact Angle). The water contact angle of the metal surfaces was measured promptly after washing. All surfaces showed an initial contact angle below 10° except Ag and Bactiguard (Table 2). The Bactiguard-coated samples were received from Bactiguard AB approximately 24 h after preparation, and the contact angles were then measured. Because of the occurrence of spontaneous adsorption of airborne pollutants (e.g., hydrocarbons) that increase the contact angle over time, all experiments were carried out within 24 h after washing.

3.2. ESCA. The total amount of surface-bound carbon was less than 25% for all surfaces (Table 3). This is generally considered a low value and thus ensures a clean surface (41). By using surfaces with such a low carbon content, we were also ensured that the chemistry of the material itself was represented in the experiments.

3.3. AFM Analyses. Micrographs from the AFM analyses of the experimental QCM-D surfaces are shown in Figure 2. The roughness of the PVD-deposited metal surfaces was found to be very low compared to that of the Bactiguard-coated surface. Root-mean-square (rms) values were less than 2 nm for the pure noble metals and 11 nm for the Bactiguard coating.

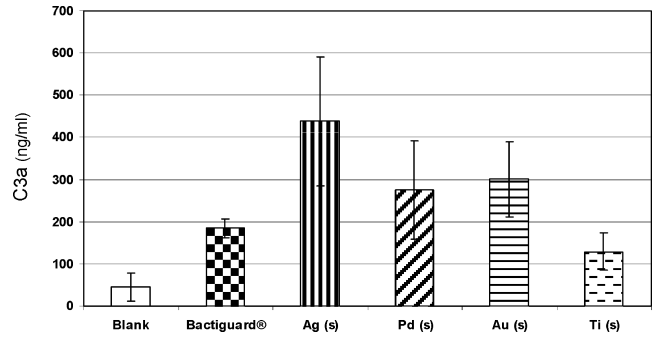

FIGURE 3. Immune complement activation measured as the amount of soluble C3a (*y* axis) found in whole blood exposed to the different noble metals. Note that Ti and the Bactiguard coating have the lowest amount of complement activation. Ti differed from Ag, Au, and Pd ($P \leq 0.05$). The Bactiguard coating differed from Ag, Au, and Ti ($P \leq 0.05$). Although not apparent to the naked eye, a difference was also found between Ag and Pd ($P \leq 0.05$). Error bars represent the standard deviation. $N \geq 4$.

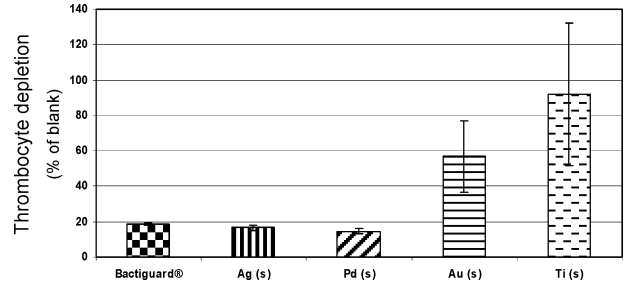

FIGURE 4. Platelet depletion from whole blood exposed to the different noble metals with unexposed blood as a reference (0% depletion). Au and Ti were highly thrombogenic compared to Pd, Ag, and the Bactiguard coating ($P \leq 0.01$). Error bars represent the standard deviation. $N \geq 5$.

3.4. Quantification of Soluble Complement Factor C3a. The combination of spontaneous bulk and surface activation of complement factor C3 results in a cleavage of C3 and hence the release of the soluble complement factor 3a (C3a). The C3a concentrations in whole blood varied after exposure to the different metals, as can be seen in Figure 3. Blood exposed to Ag showed a C3a concentration of 440 ± 200 ng/mL, followed by Au and Pd (300 ± 90 and 280 ± 100 ng/mL, respectively). The Bactiguard coating displayed a lower value (180 ± 20 ng/mL), followed by Ti (130 ± 40 ng/mL). The latter was about 3 times the amount of the blank (i.e., blood that was sampled directly and had not been exposed to any surface other than the heparinized blood collection vial), which was very low in C3a concentration (5 ± 30 ng/mL). Ti differed significantly from Ag, Au, and Pd ($P \leq 0.05$), and the Bactiguard coating differed significantly from Ag, Au, and Ti ($P \leq 0.05$). A significant difference was observed also between Ag and Pd ($P \leq 0.05$).

3.5. Depletion of Platelets in Whole Blood in Contact with Noble Metals. Whole blood that was exposed to the experimental surfaces was depleted in platelets to very different degrees, as can be viewed in Figure 4. Compared to unexposed blood (blank), Ag, Pd, and the Bactiguard coating gave rise to a small (<20%) depletion. Au and Ti were highly activating with an almost total depletion

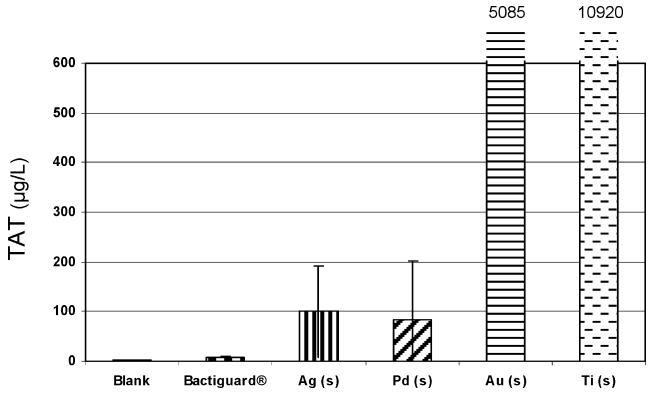

FIGURE 5. TAT generation observed in whole blood upon exposure to the different noble metals. Note that Au and Ti surfaces display very high TAT values compared to those of Ag and Pd. The TAT value of the Bactiguard coating was barely measurable. Au and Ti showed significantly higher values than Pd, Ag, and the Bactiguard coating ($P \leq 0.05$). No significant differences were observed between Pd and Ag and the Bactiguard coating. Error bars represent the standard deviation. $N \geq 4$.

(92%) as compared to the blank. Significant differences ($P \leq 0.01$) were found between all metals except between Ag and Pd. The Bactiguard coating differed significantly from Au and Ti.

3.6. Quantification of TAT. The titer of TAT was measured in whole blood exposed to different metal surfaces. Surprisingly large differences were observed between the metals, as shown by Figure 5. Ag and Pd showed low induction of TAT: 100 ± 90 and 83 ± 100 μg/L, respectively. On the contrary, Au and Ti induced high concentrations of TAT: 5100 ± 3000 and 1100 ± 900 μg/L, respectively. The Bactiguard coating showed very low TAT generation: 8.8 ± 2 μg/L. Significant differences ($P \leq 0.01$) were found between Au and Ti. No difference was found between Ag and Pd, although both differed significantly from Au and Ti, respectively. The Bactiguard coating was significantly lower than Au and Ti. A significant difference was observed between the Bactiguard coating and Ag ($P = 0.02$).

3.7. Quantification of Adsorbed Fibrinogen with QCM-D. As shown with the slide chamber model, the thrombogenicity of Ti and Au was surprisingly high in comparison to that of Ag, Pd, or the Bactiguard coating (Figures 4 and 5). Because fibrinogen is known to affect thrombogenicity and inflammation through the binding of, e.g., platelets to specific epitopes (see the Discussion section), we found it worthwhile to investigate the adsorption of fibrinogen onto the experimental surfaces. Fibrinogen adsorbed to very different degrees to the surfaces, as can be seen in Figure 6. Ag and Ti adsorbed most fibrinogen [2000 and 1600 ng/cm^2, respectively (average)] and Au and Pd moderate amounts [1400 and 1300 ng/cm^2 (average)]. The Bactiguard coating adsorbed the least fibrinogen [1000 ng/cm^2 (average)]. Also, the rapid adsorption process is obvious in Figure 6. This was found at all surfaces except on Au, where the adsorption occurred at a slightly slower rate.

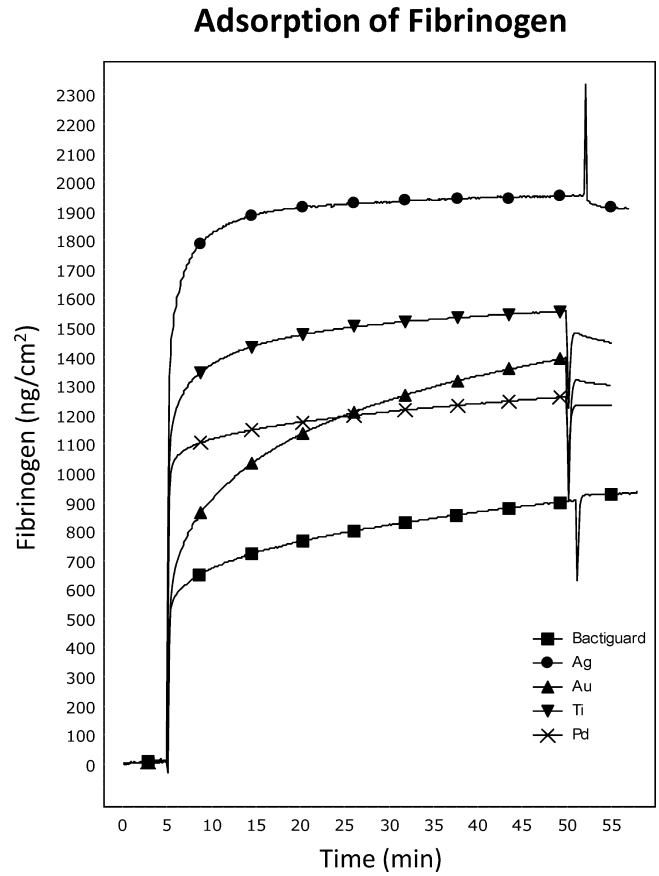

FIGURE 6. Adsorption of fibrinogen onto different noble metals and the Bactiguard coating. After a 5-min baseline check, 1 mg/mL of fibrinogen was introduced. Note the lower deposition to the Bactiguard coating. At $T = 50$ min, a rinse with a carrier buffer was performed.

4. DISCUSSION

Surface wettability is important for protein adsorption, regarding the total mass uptake and protein denaturation/conformational changes (26, 27, 42). We are well aware of the fact that any pure metal spontaneously adsorbs airborne pollutants after only a short period of time. This is demonstrated by an increase in the water contact angle over time and can be seen on our experimental surfaces as well (Table 2). One result from our careful surface cleaning procedures is high water wettability. When the experiments were carried out within hours after washing, the high wettability was maintained. As a consequence, observed differences in whole blood or single protein experiments should not originate from wettability changes but rather from different surface chemistries.

The generation of C3a in our experiments (see Figure 3) clearly demonstrates that the immune complement was activated to different degrees on different metal surfaces. However, because of the lack of time-resolved data in the slide chamber model, we are unable to distinguish the partial contribution from C3a derived via the classical or alternative pathway. There is evidence that the initial complement activation is mediated via the classical pathway, and that the alternative pathway then functions as an amplification loop, where complement proteins, mainly C3b and its degradation products, are bound to already adsorbed plasma proteins

and not to the surface itself (30). The deposition of C3b thus seems susceptible to the nature of the adsorbed protein film on top of the substrate rather than the substrate itself. This is also reported in ref 43. We have no reason to believe that the activation of the immune complement in this study is triggered in any other fashion.

The thrombin generation in whole blood varied to a large extent, as seen by the differences in TAT formation after exposure of blood plasma to the different metals (Figure 5). Because thrombin acts both on fibrinogen and directly on platelets, the correlation between platelet depletion in whole blood (Figure 4) and TAT generation (Figure 5) was expected (44). Earlier observations have indeed confirmed large TAT generation by Ti surfaces and several other metals (34), but the reasons for the differences between metals are largely unknown at this moment. The generation of thrombin on biomaterials is derived via contact activation and the intrinsic pathway (Factor XII, PK, Factor XI, and HMWK) and possibly via the extrinsic pathway (via TF) although the impact of the latter for biomaterials is still debated (31). The contribution of platelets and leukocytes to the inflammatory response at interfaces has been pointed out by several authors (22, 37), and the role of adsorbed plasma proteins and especially fibrinogen is important upon the adhesion and concomitant activation of blood cells at surfaces (45, 46). Leukocytes are known to express TF, (44) and platelets are capable of forming FXII-initiated bradykinin (47). These are cell properties that most likely affect thrombin generation and thus the subsequent thrombogenic response at biomaterials. Hence, there is a possibility that both the intrinsic and extrinsic pathways contribute here to thrombogenicity, although the upregulation of the TF gene should be a more time-consuming process than the spontaneous adsorption of coagulation Factor XII. Differences in the thrombogenicity of several metal surfaces (there among Ti) were earlier reported by Hong et al. (34). This correlates well with our data, but to our knowledge, there exist no studies where Ag or Pd was exposed to whole blood.

The adsorption of fibrinogen varied considerably between the noble metal surfaces, as can be seen in Figure 6. Despite its larger surface area and more hydrophobic nature, the Bactiguard coating adsorbed less fibrinogen than any of the pure noble metal surfaces. When the adsorption of fibrinogen onto the pure noble metals is compared with the adsorption onto the Bactiguard coating, the closest resemblance of the amount of adsorbed fibrinogen was found with Pd, although this metal was present at a very low concentration in the coating (see Table 1). If chemistry alone was the crucial parameter to decide the amount of adsorbed protein, the Bactiguard coating would have adsorbed amounts corresponding to the metal present in the highest concentration in the coating (in this instance, Ag). Because the opposite is true, we conclude that none of the noble metals in the coating can alone decide the amount of adsorbed fibrinogen to the Bactiguard coating but rather the combination of different chemistries or the nanotopography of the coating. We are unaware of previous studies on fibrinogen adsorption onto pure Ag or Pd.

The AFM analyses of our experimental surfaces (see Figure 2) confirmed a difference in the surface roughness between the Bactiguard coating and the pure noble metals on QCM-D sensors (an attempt to analyze the Bactiguard coating deposited on the PVC tubing with AFM was made but abandoned because of the softness of the PVC substrate, which interfered with the measurements). The influence of the surface nanotopography on the amount of adsorbed fibrinogen has been studied by, e.g., Rechendorff et al., (48) who reported an increase in fibrinogen adsorption with increased nanotopography on tantalum. Surprisingly, we found the opposite when the adsorption onto our pure noble metal surfaces was compared with the Bactiguard coating (see the roughness in Figure 2 with the amount of adsorbed fibrinogen in Figure 6). The nanotopography of a substrate is also known to affect the conformation of the adsorbed fibrinogen, as reported in, e.g., refs 23 and 25.

The binding and activation of platelets at biomaterial surfaces are known to be intimately associated with the adsorption of fibrinogen (49, 50), and as mentioned earlier, it is known that fibrinogen can undergo conformational changes when adsorbed to substrates with varying chemistries or topography (14, 15, 25). When the conformation of the protein is altered upon adsorption, certain epitopes on the molecule become exposed, epitopes that usually are obscure in the soluble state of the protein (17, 46, 51). The epitopes are recognized primarily by the platelet-specific receptor $\alpha_{IIb}\beta_3$, to which platelets bind and become activated (52). Thus, depending on the conformational state of the protein, the binding of cells is either promoted or impeded (16, 17, 53). Surface-located integrins for fibrinogen epitopes and other plasma proteins are also found on other cells, including a number of known pathogenic bacteria (54, 55).

In our experiments, Ag and Ti both adsorbed the highest amount of fibrinogen of the metals tested (see Figure 6) but showed very different platelet depletion and TAT generation (Figures 4 and 5). On the other hand, Au adsorbed a considerably smaller amount of fibrinogen but showed a high level of platelet depletion and TAT generation in the experiments in the slide chamber. Clearly, the amount of adsorbed fibrinogen on our experimental surfaces did not correspond to the thrombogenic response as seen in the slide chamber experiments. Thus, if only the *adsorbed mass* of fibrinogen is relied upon in the evaluation of blood compatibility, the thrombogenicity of, e.g., Ag could be greatly overestimated and, conversely, that of Au underestimated. A tentative but possible explanation of the differences in platelet depletion from whole blood seen in our experiments (Figure 4) is that the chemistry of the pure noble metal surfaces induces conformational changes to fibrinogen that would affect the ability of platelets to bind to important epitopes on fibrinogen. This is, however, yet to be confirmed by an ongoing study in our laboratory. Interestingly, the Bactiguard coating both adsorbed a low amount of fibrinogen *and* gave rise to low thrombogenic

responses in the slide chamber. Whether this is a result of the low amount of adsorbed proteins or by conformational changes of the adsorbed proteins induced by the combined chemistry or topography of the coating cannot, however, be concluded from the results in this study.

It should be noted that the composition of the Bactiguard coating differs when applied to the QCM-D sensors and the PVC tubing in this study, especially regarding the amount of Pd (see Table 1). This is probably due to the differences in the substrate chemistry, which can affect the deposition of the coating. However, in a parallel experiment in the slide chamber, the Bactiguard-coated PVC tubing was compared to the same PVC tubing that was not coated. When the coating was applied, the amount of platelet depletion as well as the generation of TAT and C3a was decreased, confirming the significance of the coating (data not shown).

Taken together, the immune complement activation and the cellular response in our study (platelet depletion) could be a secondary feature, depending on how the material's chemistry or nanotopography affects the adsorption and conformational state of proteins. Hence, an important factor to determine during evaluation of the haemocompatibility of a material is maybe therefore not necessarily *how much* but rather *how* proteins are adsorbed to a surface.

5. CONCLUSIONS

Different pure noble metal chemistries affect the coagulation of whole blood in vitro, activation of the immune complement system, and adsorption of fibrinogen differently. However, none of the individual noble metals, Ag, Au, and Pd, can alone explain the low coagulation and immune complement response on the Bactiguard commercial surface. A synergistic effect of the chemistries, nanogalvanic effects, and nanostructure per se may be a likely explanation.

Acknowledgment. The authors acknowledge Bactiguard AB for financing this research project and Helen Karlholm and Billy Södervall at Bactiguard AB for laboratory support. We also thank Bo Thunér at Linköping University for his expertise in the PVD of metals.

REFERENCES AND NOTES

(1) Branemark, P. I. *J. Prosthet. Dent.* **1983**, *50* (3), 399–410.
(2) Saint, S.; Elmore, J. G.; Sullivan, S. D.; Emerson, S. S.; Koepsell, T. D. *Am. J. Med.* **1998**, *105* (3), 236–241.
(3) Silver, S.; Phung le, T.; Silver, G. *J. Ind. Microbiol. Biotechnol.* **2006**, *33* (7), 627–34.
(4) Bosetti, M.; Masse, A.; Tobin, E.; Cannas, M. *Biomaterials* **2002**, *23* (3), 887–92.
(5) Hornez, J. C.; Lefevre, A.; Joly, D.; Hildebrand, H. F. *Biomol. Eng.* **2002**, *19* (2−6), 103–17.
(6) Turner, N.; Armitage, M.; Butler, R.; Ireland, G. *Cell Biol. Int.* **2004**, *28* (7), 541–7.
(7) Locci, P.; Marinucci, L.; Lilli, C.; Belcastro, S.; Staffolani, N.; Bellocchio, S.; Damiani, F.; Becchetti, E. *J. Biomed. Mater. Res.* **2000**, *51* (4), 561–568.
(8) Shukla, R.; Bansal, V.; Chaudhary, M.; Basu, A.; Bhonde, R. R.; Sastry, M. *Langmuir* **2005**, *21* (23), 10644–54.
(9) Merchant, B. *Biologicals* **1998**, *26* (1), 49–59.
(10) Karchmer, T. B.; Giannetta, E. T.; Muto, C. A.; Strain, B. A.; Farr, B. M. *Arch. Intern. Med.* **2000**, *160* (21), 3294–3298.
(11) Harter, C.; Salwender, H. J.; Bach, A.; Egerer, G.; Goldschmidt, H.; Ho, A. D. *Cancer* **2002**, *94* (1), 245–51.
(12) Chiang, W.-C.; Hilbert, L. R.; Schroll, C.; Tolker-Nielsen, T.; Møller, P. *Electrochim. Acta* **2008**, *54* (1), 108–115.
(13) Chang, Q. Y.; Yan, L. Z.; Chen, M. X.; He, H.; Qu, J. H. *Langmuir* **2007**, *23* (22), 11197–11199.
(14) Roach, P.; Farrar, D.; Perry, C. C. *J. Am. Chem. Soc.* **2005**, *127* (22), 8168–73.
(15) Hemmersam, A. G.; Foss, M.; Chevallier, J.; Besenbacher, F. *Colloids Surf. B* **2005**, *43* (3−4), 208–15.
(16) Wu, Y.; Simonovsky, F. I.; Ratner, B. D.; Horbett, T. A. *J. Biomed. Mater. Res. A* **2005**, *74* (4), 722–38.
(17) Hu, W. J.; Eaton, J. W.; Ugarova, T. P.; Tang, L. *Blood* **2001**, *98* (4), 1231–8.
(18) Rodrigues, S. N.; Goncalves, I. C.; Martins, M. C.; Barbosa, M. A.; Ratner, B. D. *Biomaterials* **2006**, *27* (31), 5357–67.
(19) Tang, L.; Hu, W. *Expert Rev. Med. Devices* **2005**, *2* (4), 493–500.
(20) Jung, S. Y.; Lim, S. M.; Albertorio, F.; Kim, G.; Gurau, M. C.; Yang, R. D.; Holden, M. A.; Cremer, P. S. *J. Am. Chem. Soc.* **2003**, *125* (42), 12782–6.
(21) Holmberg, M.; Stibius, K. B.; Larsen, N. B.; Hou, X. L. *J. Mater. Sci.: Mater. Med.* **2008**, *19* (5), 2179–2185.
(22) Tang, L.; Eaton, J. W. *J. Exp. Med.* **1993**, *178* (6), 2147–56.
(23) Denis, F. A.; Hanarp, P.; Sutherland, D. S.; Gold, J.; Mustin, C.; Rouxhet, P. G.; Dufrene, Y. F. *Langmuir* **2002**, *18* (3), 819–828.
(24) Song, W.; Chen, H. *Chin. Sci. Bull.* **2007**, *52* (23), 3169–3173.
(25) Roach, P.; Farrar, D.; Perry, C. C. *J. Am. Chem. Soc.* **2006**, *128* (12), 3939–45.
(26) Sigal, G. B.; Mrksich, M.; Whitesides, G. M. *J. Am. Chem. Soc.* **1998**, *120* (14), 3464–3473.
(27) Sethuraman, A.; Han, M.; Kane, R. S.; Belfort, G. *Langmuir* **2004**, *20* (18), 7779–7788.
(28) Elwing, H. *Biomaterials* **1998**, *19* (4−5), 397–406.
(29) Lord, M. S.; Cousins, B. G.; Doherty, P. J.; Whitelock, J. M.; Simmons, A.; Williams, R. L.; Milthorpe, B. K. *Biomaterials* **2006**, *27* (28), 4856–62.
(30) Wettero, J.; Askendal, A.; Bengtsson, T.; Tengvall, P. *Biomaterials* **2002**, *23* (4), 981–91.
(31) Gorbet, M. B.; Sefton, M. V. *Biomaterials* **2004**, *25* (26), 5681–703.
(32) Andersson, M. *Biosens. Bioelectron.* **2005**, *21*, 79–86.
(33) Gros, P.; Milder, F. J.; Janssen, B. J. C. *Nat. Rev. Immunol.* **2008**, *8* (1), 48–58.
(34) Hong, J.; Azens, A.; Ekdahl, K. N.; Granqvist, C. G.; Nilsson, B. *Biomaterials* **2005**, *26* (12), 1397–403.
(35) Monroe, D. M.; Hoffman, M. *Arterioscler., Thromb., Vasc. Biol.* **2006**, *26* (1), 41–48.
(36) Dahlgren, C.; Sundquist, T. *J. Immunol. Methods* **1981**, *40*, 171–179.
(37) Hong, J.; Nilsson Ekdahl, K.; Reynolds, H.; Larsson, R.; Nilsson, B. *Biomaterials* **1999**, *20* (7), 603–11.
(38) Ekdahl, K. N.; Nilsson, B.; Pekna, M.; Nilsson, U. R. *Scand. J. Immunol.* **1992**, *35* (1), 85–91.
(39) Sauerbrey, G. *Z. Phys.* **1959**, *155*, 206–222.
(40) Hook, F.; Voros, J.; Rodahl, M.; Kurrat, R.; Boni, P.; Ramsden, J. J.; Textor, M.; Spencer, N. D.; Tengvall, P.; Gold, J.; Kasemo, B. *Colloids Surf. B* **2002**, *24* (2), 155–170 .
(41) Wälivaara, B.; Aronsson, B.-O.; Rodahl, M.; Lausmaa, J.; Tengvall, P. *Biomaterials* **1994**, *15* (10), 827–834.
(42) Xu, L.-C.; Siedlecki, C. A. *Biomaterials* **2007**, *28* (22), 3273–3283.
(43) Andersson, J.; Ekdahl, K. N.; Lambris, J. D.; Nilsson, B. *Biomaterials* **2005**, *26* (13), 1477–85.
(44) Coughlin, S. R. *Nature* **2000**, *407* (6801), 258–264.
(45) Flick, M. J.; Du, X.; Witte, D. P.; Jirouskova, M.; Soloviev, D. A.; Busuttil, S. J.; Plow, E. F.; Degen, J. L. *J. Clin. Invest.* **2004**, *113* (11), 1596–606.
(46) Ugarova, T. P.; Yakubenko, V. P. Recognition of fibrinogen by leukocyte integrins. *Fibrinogen*; Annals of the New York Academy of Sciences, 2001; Vol. 936, pp 368−385.
(47) Johne, J.; Blume, C.; Benz, P. M.; Pozgajova, M.; Ullrich, M.; Schuh, K.; Nieswandt, B.; Walter, U.; Renne, T. Platelets promote coagulation factor XII-mediated proteolytic cascade systems in plasma. *1st International Conference on Exploring the Future of Local Vascular and Inflammatory Mediators, Lung, Sweden, May 26−28, 2005*; FEB, 2006; Biological Chemistry, Vol. 387, issue 2, pp 173–178.
(48) Rechendorff, K.; Hovgaard, M. B.; Foss, M.; Zhdanov, V. P.; Besenbacher, F. *Langmuir* **2006**, *22* (26), 10885–8.

(49) Farrell, D. H.; Thiagarajan, P.; Chung, D. W.; Davie, E. W. *Proc. Natl. Acad. Sci. U.S.A.* **1992**, *89* (22), 10729–10732.
(50) Grunkemeier, J. M.; Tsai, W. B.; McFarland, C. D.; Horbett, T. A. *Biomaterials* **2000**, *21* (22), 2243–2252.
(51) Clarke, M. L.; Wang, J.; Chen, Z. *J. Phys. Chem. B* **2005**, *109* (46), 22027–35.
(52) Podolnikova, N. P.; Yakubenko, V. P.; Volkov, G. L.; Plow, E. F.; Ugarova, T. P. *J. Biol. Chem.* **2003**, *278* (34), 32251–8.
(53) Weber, N.; Wendel, H. P.; Kohn, J. *J. Biomed. Mater. Res. A* **2005**, *72* (4), 420–7.
(54) Foster, T. J.; Hook, M. *Trends Microbiol.* **1998**, *6* (12), 484–8.
(55) Jarvis, R. A.; Bryers, J. D. *J. Biomed. Mater. Res. A* **2005**, *75* (1), 41–55.

AM900028E